

<https://doi.org/10.48047/AFJBS.6.6.2024.6694-6726>



African Journal of Biological Sciences

Journal homepage: <http://www.afjbs.com>



Research Paper

Open Access

Early detection of diabetes using a novel electrochemical sensor based on miRNA

Elahe Rezaei poor mashizi¹, Mahmood Dehghani Ashkezari², Navid, Nasirizadeh³, Seyed Morteza seifati⁴

¹Molecular Genetic researcher, Ashkezar Branch, Islamic Azad University Ashkezar, Yazd, Iran

²Department of Biology Medical Biotechnology Research center Ashkezar Branch, Islamic Azad university Ashkezar, Yazd, Iran

³Associate Professor Department of Polymer & textile engineering, Yazd Branch, Islamic Azad university

⁴Department of Biology Medical Biotechnology Research center Ashkezar Branch, Islamic Azad university Ashkezar, Yazd, Iran

Article History

Volume 6, Issue 6, 2024

Received: 03 Feb 2024

Accepted: 06 Apr 2024

doi:[10.48047/AFJBS.6.6.2024.6694-6726](https://doi.org/10.48047/AFJBS.6.6.2024.6694-6726)

Abstract

In this research, for the first time a novel technique was presented for early detection of diabetes based on an electrochemical sensor fabricated by modifying a screen printed carbon electrode with graphene oxide, gold nanourchin, and thiol-probes (hematoxylin) for target molecules. During the fabrication of this nanosensor, parameters such as graphene oxide concentration, gold nanourchin concentration, stabilization method, probe concentration, probe fixation time at the electrode surface, hematoxylin concentration, hematoxylin accumulation time and hybridization process were studied and optimized. The specific function of the designed biosensor versus the target miRNA was explored. The performance of the proposed sensor was evaluated in miRNA detection, so that the designed sensor was capable of detecting target miRNA in the linear range of 0.2-800 pM and with a detection limit of 0.05 pM. Also, the suggested biosensor has a very high specificity in detecting miRNA target (miR-200b) in presence of complementary miRNAs, as well as miRNAs with a different base from the target molecule and also from the miR-29a-3b as non-complementary miRNA.

Keywords: DNA biosensor, Early detection, Diabetes, miRNA, Electrochemical.

Introduction

Diabetes is a chronic disease in which the amount of insulin secretion is less than values needed to balance sugar (glucose) in the blood. It should be noted that the main role of insulin is to help the metabolism of starches and simple sugars, thus regulating blood sugar; hence, a relative decrease in the course of diabetes leads to an increase in blood sugar [1]. This phenomenon, if not controlled and adjusted properly, leads to irreparable damage to various parts of the body. This defect (relative reduction in insulin levels) prevents effective usage of glucose and prevents storing of blood sugar levels [2]. As a result, the amount of glucose or so-called blood sugar in affected people is increased, this complication can lead to cardiovascular, renal, eye and nerve diseases, as well as to the occurrence of various complications in afflicted patients [3]. Therefore, monitoring and early detection of diabetes in high-risk individuals is very important. This latent disease can occur at any age from childhood to adulthood and accompany the patient for a lifetime. The main challenge in controlling and preventing diabetes is early detection of the disease, which may provide a tremendous opportunity for recovery and treatment in people with diabetes [4]. One of the easiest ways to diagnose this disease is to measure the level of glucose (sugar) in the blood, which has become one of the main priorities of medical research and so far a variety of methods and devices have been used [5]. There are many techniques employed, including chromatography [6], fluorescence [7], calorimetry [8], infrared spectroscopy [9], and electrochemistry [10-11]. The electrochemical sensors have been more welcomed by researchers due to their high sensitivity, excellent selectivity, low cost, fast response, low analytical requirements, easy use and appropriate diagnostics [12-13].

Electrochemical sensors developed to measure glucose generally fall into two categories: enzymatic and non-enzymatic [14]. The mechanism of non-enzymatic sensors is based on direct oxidation of glucose, and in most cases the electrodes used are modified with different nanoparticles. However, in the enzymatic ones, the glucose oxidase as enzyme is used to accelerate the oxidation of glucose and to measure the levels of glucose by measuring the hydrogen peroxide produced during the reduction process [15].

Simultaneous with the development of nanotechnology and advances in the production of various nanoparticles, this technology entered the field of electrochemical sensors to improve accuracy, increase selectivity and sensitivity. The unique properties of nanoparticles (whether organic or inorganic) such as high surface-to-volume ratio, catalytic performance and improved mass-electron transfer cause great improvement in the effective surface area, electron transfer rate and electrode sensitivity to the species being measured [16].

Graphene oxide has attracted the attention of many researchers due to its prominent physical and chemical properties, excellent catalytic activity and low production cost for designing and manufacturing a new generation of chemical and biological sensors [17]. The use of graphene derivatives has improved the performance and progress in the field of production and improved the properties of biosensors, due to their unique properties in the

field of optimal electrical conductivity, flexibility, lightness and good strength. Due to the two-dimensional plate structure, this organic matter has improved the linear range and the optimal relationship between concentration and redox signal. The detection limit, the sensitivity and its response time are other factors that the use of graphene has enhanced [18]. On the other hand, gold nanoparticles are the most widely used metal nanoparticles in the manufacture of enzymatic biosensors. These nanoparticles improve electron transfer between the active site of redox proteins and the electrode surface. The use of gold nanoparticles on the electrode surface increases the electron transfer rate constant between glucose oxidase and substrate in glucose detection [19]. These nanoparticles have good biocompatibility, therefore, the enzyme is well stabilized on Au nanoparticles and maintains its activity. On the other hand, due to the high electrical conductivity of gold, direct electronic contact between the active sites and the electrode surface is also possible [20].

In recent years, the use of MicroRNAs (miRNAs) as diagnostics biomarkers for the detection of disease and gene mutations has been considered by researchers. They are a class of small non-coding RNAs with 20–24 nucleotides which play an important role in regulating gene expression. In literature stated that miR-375 plays a direct role in insulin secretion and pancreatic islet development by targeting the pancreatic genes; insulin, myotrophin and phosphoinositide-dependent protein kinase-1. Analysis of miR-375 level in first degree relatives of T2DM patients may provide insights on importance of miR-375 as a potential biomarker for the early prediction of T2DM among high-risk individuals [21].

Studies have shown that Au/Graphene based on nanohybrid biosensors increase biocompatibility and measurement sensitivity. Although numerous research has been reported on electrode modification by various nanomaterials to improve the performance of DNA biosensors, nanomaterial preparation or electrode modification strategies are often complex; in addition, some nanomaterials still have limitations to improve the performance of DNA biosensors [22-23].

In this study, a new electrochemical sensor based on screen printed carbon electrode modified by graphene oxide/gold nanourchin/dsDNA (dsDNA/GNU/GO/SPCE) is introduced for rapid and accurate detection of glucose among people suspected to have diabetes. The GO has been used as the first layer to increase the surface area of the electrode and stabilize the subsequent layers. GNU also play an important role in increasing electrical conductivity and accelerating electron transfer rate, increasing catalytic activity of the sensor as well as stabilizing used oligonucleotide sequences in electrochemical detection.

Experimental

Chemicals

The characteristics of the chemicals used in this study are summarized in Table 1.

Table 1

Electrochemical instrumentation

The whole range of electrochemical studies, including cyclic voltammetry (CV), differential pulse voltammetry (DPV) and electrochemical impedance spectroscopy (EIS) were implemented with Autolab potentiostat/galvanostat PGSTAT101 (M101) from Metrohm Company (Netherland) at laboratory temperature (25 ± 1 °C). The interface program was GPES version 4.9 on a personal computer, and screen-printed carbon electrode (SPCE) from DropSens Company (Spain) was used instead of the conventional three electrode system. The SPCE as working electrode was made of carbon (4 mm diameter), the counter electrode was made of platinum and the reference electrode was made of silver.

Oligonucleotides

The sequence of miR-375 was obtained from a previous SELEX study of our research team. All oligonucleotides were synthesized, HPLC-purified and received in lyophilized form by Metabion Company (Germany) with the following sequences:

5-GCGACGAGCCCCUCGCACAAACC-3

ssProbe: 5'-Thiol:

Preparation of biosensor

The electrochemical biosensor was developed by DNA hybridization based on the self-assembled monolayer (SAM) technique. Here, a screen-printed carbon electrode (SPCE) surface was cleaned and washed with ethanol/purified water (1:1). Then, a drop of 4.0 μ L of dispersed GO solution (3.0 mg/mL) was placed on the SPCE and dried in a humid chamber for 60 min (scheme 1) (GO/SPCE). After washing with distilled water, a drop of 4.0 μ L of AuNP dispersion (1 mg/mL) was poured on the modified electrode and was kept at room temperature to be dried slowly (AuNP/GO/SPCE).

Next, a 4.0 μ L droplet of the immobilization buffer solution with pH 4.5 containing 10.0 nM of the thiolated single strand probes was dropped on the modified electrode surface and for the attachment of the probes onto the AuNP surface, was incubated in a high-humidity container at ambient temperature for 120 min (ssDNA/AuNPs/GO/SPCE). The electrode was immersed in 0.1 mM MCH solution for 2 min to block the remaining bare regions on the surface of AuNPs. The resulting modified electrode was rinsed with (80:20 v/v) ethanol, water and distilled water, respectively. In the end, the prepared electrode was dipped in the hybridization buffer solution (pH 7.0) containing 1.0 nM concentration of the complementary miRNA, 0.05 M phosphate and 0.3 M SC at room temperature (25 ± 1 °C) for 120 min (dsDNA/AuNP/GO/SPCE).

Finally, in this stage, the biosensor was ready for electrochemical experiments. Then the biosensor was incubated into the desired concentrations of the miR-375 for 120 min. To accurately evaluate the modifications on the SPCE during the fabrication process, after every preparation, the analysis of CV and EIS was carried out in the solution of 1.0 mM $K_3[Fe(CN)_6]/K_4[Fe(CN)_6]$ containing 1.0 M KCl. The potential range of CV was -0.025 to 0.33 V with a sweep rate of 0.02 V/s, and EIS was performed from 100 kHz to 0.01 Hz with amplitude of 5 mV and potential of 0.27 V. Additionally, the electrochemical signal

measurements were done using differential pulse voltammetry (DPV), with a modulation time of 0.05 s, amplitude of 25 mV and step potential of 50 mV in 0.1 M PBS buffer (pH 7.0). All steps of the preparation of this sensor are shown in scheme (1).

Scheme 1

Optimization

The fabrication procedure of biosensor consists of several different stages, in which various parameters affect the sensor response. Here, immobilization method of a single strand probe, incubation time and concentration of the probe, hybridization method, the incubation time and concentration of the Hem were chosen and their effects on the response of sensor were studied.

Immobilization of a single strand probe on modified electrodes was performed by two conventional methods, namely self-arrangement of DNA in solution and self-arrangement of DNA by small drop of thiolate DNA, and the results of both methods were compared. In the first method, electrodes were modified with graphene oxide and gold nanourchin and placed in a buffer containing 0.1 μ M DNA for 0.2 hours, until a single strand (SS-probe) thiol was self-arranged on the surface of the electrode. In the second method, 2.5 μ L of a buffer solution containing 0.1 μ M of probe was dropped on the electrode surface and then transferred to a supersaturated steam bath at ambient temperature for 2 h and allowed to stabilize the thiol single strand (probe). After the stabilization process, the self-assembled electrodes with the probe were first cleaned with a washing solution (solution containing 0.05 M phosphate buffer and 0.3 M NaCl with a pH = 7.0) and then immersed in a solution 1.0 mM MCH for 2 minutes and then washed with 80:20 ethanol-water solution. The resulting electrodes were placed in a 0.1 M phosphate buffer with pH 7.0 containing 0.1 mM HEM for 5 minutes. Consequently, these electroactive species were accumulated on the ss-DNA/GNU/GO/SPCE. Then the electrode was transferred to the electrochemical cell and the differential pulse voltammogram of the Hem accumulated on the surface of the electrode was used as a measure of the stabilization rate of the thiol probe.

In addition, the other parameters of the biosensor and its preparing process included accumulation time of SS-DNA (10 -120 min), probe concentration (50.0 – 120.0 nM), Hem concentration (0.02 – 0.2 mM) and accumulation time of Hem (1-8 min), which were serially optimized to reach the best miRNA sensing performance. The reduction signal of accumulated Hem on the hybridized SS-Probe-Target miRNA was assumed as the dependent variable for all optimization experiments.

Detection of miRNA

The prepared biosensor was incubated for 120 min in the desired concentration of target miRNA solution in the hybridization buffer, and then gently rinsed with the washing solution. Afterwards, it was immersed in the Hem solution for 5 min on a stirrer with very slow rotation for better accumulation of Hem on the resulted hybrid of SS-probe-miRNA via intercalation. For control, the prepared biosensor was directly immersed in a Hem solution

without hybridization with target miRNA, and the resulted DPVs were compared with the voltammograms of the target-hybridized biosensor.

Scanning electron microscope (SEM) analysis

The SEM imaging analysis of the working electrode surface during fabrication of nanosensor was performed using field emission scanning electron microscopy (FE-SEM) MIRA 3-XMU (Tescan, Japan).

3. Results and discussion

3.1. Morphology of developed nanosensor

Fig. 1A and B depict TEM image of GO and GNU. As demonstrated in the figure, GO and GNU have a wrinkled layer structure, a multiple-branch shape and a uniform size, respectively.

The modification steps of SPCE with GO and GNU was monitored for the preparation of electrochemical biosensor by scanning electron microscopy. The SEM micrographs of the SPCE modified with either of GO or GO/ GNU, along with their elemental analysis, are shown in Figure 1. As can be seen in Fig. 1C, the surface of the SPCE is roughened by the immobilizing of GO sheets, and the GO-plate-structure is observable at the electrode surface. Some researchers believe that the fixation of GO nano sheets enhances the effective surface area of the electrodes [24-25].

The stabilization of GNU on the surface of the SPCE is also well-illustrated in Fig 1D. Therefore, due to the excellent conductivity properties of gold nanourchin, it is expected to improve the rate of electron transfer from the electrode surface [26], and consequently, enhancing the sensitivity of the electrode to miRNA.

EDX analysis of the surface of the (GNU/GO/SPCE) electrode is also illustrated in Fig. 1E. As the figure shows, 47.3 % of nanosensor surface elements are gold, and carbon (42.5 %) and oxygen (10.2 %) are other constituents of the nanosensor surface. Fig. 1 F-H show the elemental mapping of GNP, carbon and oxygen elements deposited on SPCE, in order to investigate their localized elemental information, which shows that elements of gold and carbon were well immobilized and almost uniformly distributed on the surface of SPCE.

Figure. 1.

Electrochemical characterization of proposed biosensor

In order to evaluate the accuracy of the fabrication and preparation steps of the biosensor, cyclic voltammograms of different electrodes in 0.1 mM $K_3 [Fe(CN)_6]$ in phosphate with a pH 7.0 after electrode modification were recorded and compared. Fig. 2 shows the cyclic voltammograms of the electrode in 0.1 mM $[Fe(CN)_6]^{3-/4-}$ in 0.1 M KCl for SPCE bare electrode (voltammogram a), GO/SPCE (voltammogram b), GNU/ GO/SPCE

(voltammogram c), MCH/ssDNA/GNU/GO/SPCE (voltammogram d) and dsDNA/GNU/GO/SPCE (voltammogram e).

As can be seen in voltammogram a, the bare SPCE in 0.1 mM $K_3[Fe(CN)_6]$ in phosphate buffer with pH 7 has an ideal current. Such a voltammogram indicates the fast electron transfer rate at electrode surface. In comparison to the performance of the bare SPCE, the modified GO/SPCE has a lower peak current, but the GNU/GO/GCE displayed a significant increase in peak current. The decline of the current by addition of the GO, is because of the negative charge of the GO in solution, which interacted with $[Fe(CN)_6]^{3-/4-}$ ions due to the ionized functional groups, or the GO acted as an insulating layer, which have been reported in publications before [25-26]. On the other hand, GO has been defined as a weak conductor of electricity, which due to the significant increase at surface through presence of conductive nanoparticles, this defect is largely eliminated.

Due to the presence of GNU, the signals of cathodic and anodic peaks related to the oxidation and reduction of electroactive species $[Fe(CN)_6]^{3-/4-}$ on the surface of GNU/GO/SPCE (voltammogram c) greatly increased compared to the voltammogram of the modified electrode with GO (voltammogram b). In fact, this increase in redox peak current of $[Fe(CN)_6]^{3-/4-}$ anions demonstrate the important role of GNU in obtaining higher electrochemical signals. This phenomenon confirms that the GNU not only enriches the electrode response, but also serves as active binding sites for oligonucleotide probes by providing a larger effective surface area. Assembly of ssDNA onto the GNU/GO/SPCE surface, caused a fall in peak current, but the MCH treatment helped the decoration of the ssDNAs on the GNU, and as a result the current slightly increased (voltammogram d). In subsequent hybridization of the DNA probe with the complementary DNA, the redox peak currents decreased since the phosphate backbone of the DNA develops more negative charges on the surface electrode. These observations confirmed the assembling procedures of the modified electrodes in every stage of biosensor preparation.

Fig. 2.

Optimization of variables

GO concentration

In this section, different concentrations of GO (0.4 - 1.7 mg/mL) were placed on the SPCE for fabrication of biosensor, the results of which are shown in Figure 3. It is observed that by increasing the concentration of GO to 0.9 mg/mL, the response of the biosensor increases and then with further increase, the analytical response of the sensor drops. Thus, it can be concluded that GO as a two-dimensional plate structure has increased the effective level of the sensor and increased its analytical signal to the target probe [24].

Figure 3.

GNU concentration

In the second stage of optimization, the effect of the concentration of GNU (40-130 $\mu\text{g}/\text{mL}$) on its electrochemical response of modified SPCE to the target probe was studied, the results of which are plotted in Figure 4. As can be seen, the highest analytical signal of probe was obtained on the modified electrodes modified with 100 $\mu\text{g} / \text{mL}$ GNU. As mentioned before, gold nanourchin increased the sensitivity of the biosensor to the target probe due to its unique properties, especially its excellent conductivity [22].

Figure 4.

Probe stabilization method

Figure 5 shows that small droplet stabilization method has the best current response, and this method was used as the optimal method for immobilization of ss-DNA in other steps. Also, from the voltammograms (Figure 5), it can be easily concluded that the analytical signals attained by using the droplet self-assembly method for hybridization were larger and therefore, this method was chosen to prepare the electrode modified with the probe.

Figure 5.

Probe Concentration

In this step, in order to achieve the best suitable concentration of the probe for immobilization on the surface of GNU/GO/SPCE, solutions with different concentrations of oligonucleotide single strand (20.0 -280 nM) in the stabilization buffer were dropped on the surface of modified SPCE and then placed in a saturated steam bath system for 90 min. In this way, the process of fixation of single-strand oligonucleotide was performed and other steps were performed as in the previous sections. The diagram of oxidation current in terms of probe concentration is shown in Figure 6. As can be seen, the most suitable concentration of single-strand oligonucleotide for immobilization on the surface of GNU/GO/SPEC is 240 nM, which has the highest current rate.

Figure 6

Immobilization time of the probe

To optimize the effect of time on the fixation rate of the single-stranded probe on the surface of the modified SPCE, 4 μL thiol- probe solution in the stabilization buffer was placed on the surface of the uncoated electrode and then the electrode was placed in a supersaturated bath for 10 to 120 min. Following steps included rinsing, placing the electrode in MCH aqueous solution, accumulation of hematoxylin on the surface of the modified electrode, and its cathodic peak current was measured. Diagrams of the signal changes resulting from the oxidation of accumulated Hem on the surface of the SPCE modified with the probe in terms of the stabilization time of the probe are given in (Figure 7). As the resulting diagram shows, with increasing the stabilization time of the probe, the current initially increases and reaches its maximum value after 90 min. Next, the current of the Hem oxidation begins to decrease,

due to excessive accumulation of oligonucleotides on the electrode surface, which leads to disagreements in their placement, stabilization and placement, as well as inadequate access of hem to the electrode surface.

Figure 7 –

Concentration of Hem

The effect of Hem concentration (0.03-0.2 mM) on the analytical response of the SPCE modified with dsDNA/GNU/GO/SPCE was investigated, and the results is depicted in Figure 8. As the current changes of Hem accumulated on the ds-DNA, the best concentration of Hem for its accumulation on the surface of modified SPCE was 0.11 mM.

Figure 8 -

Immobilization time of Hem

In this stage, in order to achieve the best conditions of the Hem accumulation on ds-DNA and to further Hem accumulation at the dsDNA/GNU/GO/SPCE, the effect of the accumulation time of this electroactive detector was also evaluated, and the results are shown in Figure 9. As can be seen, the highest oxidation current of Hem was obtained in 6 min.

Figure 9

Hybridization technique

Hybridization of single-stranded probe with its complement was performed in different ways. In this study, three different methods, namely small droplet hybridization, hybridization in preheated solution and hybridization in solution were investigated. In the first method (small droplet), 4 μ L of 240 nM solution of single-stranded target was placed on the surface of dsDNA/GNU/GO/SPCE, then it was placed in a supersaturated steam bath for 90 min. Afterwards, It was placed in Hem solution and then a DPVs was plotted (voltammogram a Figure 10). In the hybridization method, using preheated solution, the solution containing 10.0 nM single strand target in the hybridization buffer was heated to 85 °C. The modified electrode with single-strand probe was then placed in the aforementioned solution for 3.0 min, and then the heating was stopped and the electrode slowly cooled down to ambient temperature. After the solution had cooled, an electrode containing double-stranded oligonucleotides was removed from the solution and placed in the wash solution. Hem was then accumulated on the surface of dsDNA/GNU/GO/SPCE and its DPV was plotted (voltammogram b Figure 10). In the third method, the modified electrode with single strand probe was placed in a solution containing 240 nM single strand target in a hybridization buffer for 90 min. After this time, the dsDNA/GNU/GO/SPCE was placed in the wash solution for some time, then it was removed and immersed in a solution containing 0.11 mM Hem for 10 min. Next the electrode was washed and finally, a DPV was drawn

(voltammogram c, Figure 10). Comparing voltammograms a, b and c shows that highest current response was observed in the modified electrode with the solution method. Accordingly, this hybridization method was used in the subsequent test.

Figure 10.

Selectivity of biosensor

Selectivity of DNA biosensor in the detection of target oligonucleotides enables the biosensor to rely on its high specificity to detect the target molecule among some of non-specific molecules and possibly with only one or more different bases [27]. Therefore, in order to evaluate the biosensor performance, the electrodes modified in the previous section were placed separately in solutions of non-complementary oligonucleotides (miR-29a-3p) with a complementary base as well as the target oligonucleotide (miR-200b). Consequently, the modified electrodes were placed in a 0.1 M phosphate buffer (pH 7.0) containing 0.11 mM Hem solution for 10 minutes, which was slowly rotating, and then DPVs of the accumulated Hem were recorded (Fig 11). In addition, DPVs of biosensor hybridized to a target miRNA without immersion in Hem solution, as well as a MCH/GNU/GO/SPCE without probe stabilization and without hybridization were examined for evaluating the function of Hem as an indicator in increasing the sensitivity of the biosensor.

Fig. 11.

As shown in Fig. 11, in comparison to the DPV response of Hem with the ssDNA modified SPCE (curve b), an increase was observed in the peak current value of Hem when the DNA probe was hybridized with its complementary sequence (curve e). The current peak obtained by probe hybridization with the mismatch DNA (curve d) was higher than the one with the non-complementary sequence (curve c). The results showed that the modified electrode had satisfactory selectivity for DNA hybridization.

Analytical performance of the nanobiosensor

Following optimization of the procedure for fabrication of biosensor, all the analytical experiments were done under the best resulted conditions and the fabricated biosensor showed great sensitivity in detection of different target miRNA concentrations in the hybridization buffer for 120 min (Fig. 12).

As the results of this figure show, in a relatively wide range of target miRNA concentrations (from 0.2 to 800 pM of miR-200b), there was a linear relationship between the accumulated cathodic current of Hem and the concentration of target complement miRNA. In fact, up to 800 pM, there are suitable sites for interaction between the thiol-probe stabilized at the electrode surface and miR-200b. At concentrations above 800 pM, the

reduction signal of the indicator decreases to a constant value, and the hybridization process is almost more difficult and then it is stopped.

The calculated detection limit was identified to be 0.05 pM, using the equation $C_m = 3s_{bl}/m$ [28], where s_{bl} is the standard deviation of 15 repeated DPV of the blank response (the signal of Hem on the nanobiosensor) and m is the slope of the calibration plot. The average voltammetry current and the precision estimated in terms of the relative standard deviation (RSD) for twelve repeated measurements ($n = 12$) of 85.0 fM of the target DNA were 495.0 ± 12.0 nA and 2.6%, respectively.

Fig. 12.

In Table 2, some of the analytical characteristics of the proposed biosensor are compared with those previously reported by others [29-37]. As it can be seen, some analytical responses such as detection limit and linear range of response are higher in some cases versus the represented works in Table 2. It is the only biosensor provided to diagnose diabetes using microRNA. Therefore, the proposed biosensor has a relatively better response than other previously published DNA biosensors, especially in response time, sensitivity and selectivity.

Table 2

In order to study the stability of the suggested sensor, GNU/GO/SPCE, immobilized by ssDNA were produced with the method described in the experimental part Section 2.3; and were kept for different time periods (days) in temperature of 4 °C in the phosphate buffer solution pH 7.0. The aforementioned modified electrodes were examined for the purpose of the measurement of target DNA sample, in the temporal range of 1 to 14 days. The results showed that the modified electrodes had the best stability for less than 3 days, and after 3 days, the Hem decomposition placed on the ss-DNA showed more than 5% decrease. In conclusion, the best stability of the electrodes immobilized by ssDNA is within 3 days' storage under the temperature of 4 °C, for the most effective use in measurements.

Real sample evaluation

The early detection and continuous monitoring of blood sugar play an important role in the treatment and prevention of diabetes [38]. The proposed nanobiosensor was used to measure miR-375 as a biomarker of diabetes in blood plasma and quantitative real-time PCR (QRT-PCR) method was used for compare the function of the developed biosensor. The real samples were obtained from blood plasma of a non-diabetic healthy human at a medical diagnostic laboratory and stored at -20 °C until testing. From that plasma sample, 20 µL was taken and diluted with 100 µL of phosphate at pH 7 and used for hybridization on ssDNA/GNU/GO/SPCE. Then, different concentrations of miR-375 were added to the diluted plasma sample. It should be noted that the concentration miR-375 in the plasma sample of a non-diabetic individual is less than the recommended sensor detection. Therefore, the initial concentration of miR-375 in the plasma sample was assumed to be zero. In order to determine

the miR-375 in plasma samples, the prepared sensors were placed in prepared solutions for accumulation of miR-375 on the modified electrodes, followed by DPV of accumulated hematoxylin, which was recorded after hybridization. Finally, the recovery rates of the concentrations added to the solutions were calculated. The measurements were repeated three times. The results are given in Table 3. As the figures in this table indicate, the proposed biosensor can be considered to be an additional test beside PCR for measurement of the miR-375 in clinical specimens without any preparation, extraction, or concentration enhancement as well as lower price and complexity and also higher sensitivity.

Table 3.

Conclusion

This research was conducted to prepare an electrochemical sensor developed for early detection of diabetes based on detection of miR-375. This biosensor efficiency was based on interactions of Hem as an electroactive DNA label at SPCE modified with GO and GNU and complementary miRNA with miR-375. The electrochemical experiments also confirmed that Hem-based DNA biosensors are capable of detecting the single-base mismatch in the target DNA. The experiments provided proof that the best method for probe self-assembly is droplet self-assembly and the best hybridization method is solution hybridization. Under optimum conditions, electrochemical signal had a linear relationship with the concentration of the target DNA ranging from 0.2 pM to 800.0 pM, and the detection limit was 0.05 pM. The great responses of the biosensor in the simulated real sample, represent its potential for use in future clinical applications for diabetes detection. Besides, our nanobiosensor, in comparison with previously published electrochemical nanobiosensors as well as conventional miRNA quantification methods, has the ease of assembly, simple detection process, and it is fast and cost-effective.

References

- [1] Nitesh Pradhan, Geeta Rani, Vijaypal Singh Dhaka, Ramesh Chandra Poonia, 14 Diabetes prediction using artificial neural network, *Deep Learning Techniques for Biomedical and Health Informatics*, Academic Press, 2020. 327-339. <https://doi.org/10.1016/B978-0-12-819061-6.00014-8>.
- [2] Swapna G., Vinayakumar R., Soman K.P., Diabetes detection using deep learning algorithms, *ICT Express*, 4 (4) 2018, 243-246. <https://doi.org/10.1016/j.ict.2018.10.005>.
- [3] Mathieu Ravaut, Hamed Sadeghi, Kin Kwan Leung, Maksims Volkovs, Kathy Kornas, Vinyas Harish, Tristan Watson, Gary F. Lewis, Alanna Weisman, Tomi Poutanen & Laura Rosella. Predicting adverse outcomes due to diabetes complications with machine learning using administrative health data. *npj Digit. Med.* 4, 24 (2021). <https://doi.org/10.1038/s41746-021-00394-8>
- [4] Suresh T. Chari, Anirban Maitra, Lynn M. Matrisian, Eva E. Shrader, Bechien U. Wu, Avinash Kambadakone, Ying-Qi Zhao, Barbara Kenner, Jo Ann S. Rinaudo, Sudhir

Srivastava, Ying Huang, Ziding Feng, Early Detection Initiative: A randomized controlled trial of algorithm-based screening in patients with new onset hyperglycemia and diabetes for early detection of pancreatic ductal adenocarcinoma, *Contemporary Clinical Trials*, 113, 2022, 106659. <https://doi.org/10.1016/j.cct.2021.106659>.

[5] Leon Kopitar, Primoz Kocbek, Leona Cilar, Aziz Sheikh & Gregor Stiglic. Early detection of type 2 diabetes mellitus using machine learning-based prediction models. *Sci Rep* 10, 11981 (2020). <https://doi.org/10.1038/s41598-020-68771-z>

[6] Qihui Xuan, Fujian Zheng, Di Yu, Yang Ouyang, Xinjie Zhao, Chunxiu Hu & Guowang Xu. Rapid lipidomic profiling based on ultra-high performance liquid chromatography–mass spectrometry and its application in diabetic retinopathy. *Anal Bioanal Chem* 412, 3585–3594 (2020). <https://doi.org/10.1007/s00216-020-02632-6>

[7] Seyyed Mojtaba Mousavi, Seyyed Alireza Hashemi, Ahmad Gholami, Sargol Mazrae doost, Wei-Hung Chiang, Omid Arjmand, Navid Omidifar, Aziz Babapoor, "Precise Blood Glucose Sensing by Nitrogen-Doped Graphene Quantum Dots for Tight Control of Diabetes", *Journal of Sensors*, 2021, 5580203, 1-14, <https://doi.org/10.1155/2021/5580203>

[8] Chunhua Lin, Yue Du, Shiqi Wang, Li Wang, Yonghai Song, Glucose oxidase@Cu-hemin metal-organic framework for colorimetric analysis of glucose, *Materials Science and Engineering: C*, 118, 2021, 111511. <https://doi.org/10.1016/j.msec.2020.111511>.

[9] Lubinski, Thorsten, Bartosz Plotka, Sergius Janik, Luca Canini, and Werner Mäntele. "Evaluation of a Novel Noninvasive Blood Glucose Monitor Based on Mid-Infrared Quantum Cascade Laser Technology and Photothermal Detection." *Journal of Diabetes Science and Technology* 15, no. 1 (January 2021): 6–10. <https://doi.org/10.1177/1932296820936634>.

[10] Lucas Patricio Hernández-Saravia, Tamara Martinez, Jaime Llanos, Mauro Bertotti, A Cu-NPG/SPE sensor for non-enzymatic and non-invasive electrochemical glucose detection, *Microchemical Journal*, 160, A, 2021, 105629. <https://doi.org/10.1016/j.microc.2020.105629>.

[11] Bingul Kurt Urhan, Umit Demir, Tuba Oznuluer Ozer, Hulya Ozturk Dogan, Electrochemical fabrication of Ni nanoparticles-decorated electrochemically reduced graphene oxide composite electrode for non-enzymatic glucose detection, *Thin Solid Films*, 693, 2020, 137695. <https://doi.org/10.1016/j.tsf.2019.137695>.

[12] Shahab Maghsoudi, Arman Mohammadi, Reduced graphene oxide nanosheets decorated with cobalt oxide nanoparticles: A nonenzymatic electrochemical approach for glucose detection, *Synthetic Metals*, 269, 2020, 116543. <https://doi.org/10.1016/j.synthmet.2020.116543>.

[13] Dehghani, M., Nasirizadeh, N., Yazdanshenas, M. E. Determination of cefixime using a novel electrochemical sensor produced with gold nanowires/graphene oxide/electropolymerized molecular imprinted polymer. *Mater. Sci. Eng. C*. 96 (2019) 654-660. <https://doi.org/10.1016/j.msec.2018.12.002>.

[14] Jie Zhang, Yudong Sun, Xianchun Li, Jiasheng Xu, Fabrication of NiCo₂O₄ nanobelt by a chemical co-precipitation method for non-enzymatic glucose electrochemical sensor application, *Journal of Alloys and Compounds*, 831, 2020, 154796. <https://doi.org/10.1016/j.jallcom.2020.154796>.

[15] Hassan, Mohamed H., Cian Vyas, Bruce Grieve, and Paulo Bartolo. 2021. "Recent Advances in Enzymatic and Non-Enzymatic Electrochemical Glucose Sensing" *Sensors* 21, no. 14: 4672. <https://doi.org/10.3390/s21144672>

[16] Somayeh Tajik, Hadi Beitollahi, Sayed Zia Mohammadi, Mostafa Azimzadeh, Kaiqiang Zhang, Quyet Van Le, Yusuke Yamauchi, Ho Won Jang and Mohammadreza Shokouhimehr, Recent developments in electrochemical sensors for detecting hydrazine with different modified electrodes. *RSC Adv.*, 2020, 10, 30481-30498. <https://doi.org/10.1039/D0RA03288C>.

[17] Seyyed Alireza Hashemi, Seyyed Mojtaba Mousavi, Sonia Bahrani, Seeram Ramakrishna, Integrated polyaniline with graphene oxide-iron tungsten nitride nanoflakes as ultrasensitive electrochemical sensor for precise detection of 4-nitrophenol within aquatic media, *Journal of Electroanalytical Chemistry*, 873, 2020, 114406. <https://doi.org/10.1016/j.jelechem.2020.114406>.

[18] Samaneh Nazerdeylami, Jahan B. Ghasemi & Alireza Badiei (2020) Anthracene modified graphene oxide-silica as an optical sensor for selective detection of Cu²⁺ and I⁻ ions, *International Journal of Environmental Analytical Chemistry*, 100:6, 686-701, DOI: 10.1080/03067319.2019.1638919.

[19] Farnaz Bahavarnia, Ahmad Mobed, Mohammad Hasanzadeh, Arezoo Saadati, Soodabeh Hassanpour, Ahad Mokhtarzadeh, Bio-assay of *Acintobacter baumannii* using DNA conjugated with gold nano-star: A new platform for microorganism analysis, *Enzyme and Microbial Technology*, 133, 2020, 109466. <https://doi.org/10.1016/j.enzmictec.2019.109466>.

[20] Roozbeh Siavash Moakhar, Tamer AbdelFatah, Alireza Sanati, Mahsa Jalali, Sarah Elizabeth Flynn, Sahar Sadat Mahshid, and Sara Mahshid. A Nanostructured Gold/Graphene Microfluidic Device for Direct and Plasmonic-Assisted Impedimetric Detection of Bacteria. *ACS Appl. Mater. Interfaces* 2020, 12, 20, 23298–23310. <https://doi.org/10.1021/acsami.0c02654>.

[21] Jafari, S., Dehghani, M., Nasirizadeh, N., Azimzadeh, M. An azithromycin electrochemical sensor based on an aniline MIP film electropolymerized on a gold nanourchins/graphene oxide modified glassy carbon electrode, *J. Electroanal. Chem.* 829 (2018) 27-34. <https://doi.org/10.1016/j.jelechem.2018.09.053>.

[22] Golkarieh, A.M., Nasirizadeh, N., Jahanmardi, R. 2021. Fabrication of an electrochemical sensor with Au nanorods-graphene oxide hybrid nanocomposites for in situ measurement of cloxacillin, *Materials Science and Engineering: C*, 118, 2021, 111317. <https://doi.org/10.1016/j.msec.2020.111317>.

[23] Azimzadeh, M., Nasirizadeh, N., Rahaie, M., Naderi-Manesh, H. Early detection of Alzheimer's disease using a biosensor based on electrochemically-reduced graphene oxide and gold nanowires for the quantification of serum microRNA-137. *RSC Adv.* 7(88) (2017) 55709-55719. <https://doi.org/10.1039/C7RA09767K>.

[24] Seifati, S.M., Nasirizadeh, N., Azimzadeh, M., Nano-biosensor based on reduced graphene oxide and gold nanoparticles, for detection of phenylketonuria-associated DNA mutation. *IET Nanobiotechnol.* 12(4) (2017) 417-422. <http://dx.doi.org/10.1049/iet-nbt.2017.0128>

[25] Aghili, Z., Nasirizadeh, N., Divsalar, A., Shoeibi, S., Yaghmaei, P. A nanobiosensor composed of Exfoliated Graphene Oxide and Gold Nano-Urchins, for detection of GMO products. *Biosens. Bioelectron.* 95 (2017) 72-80. <https://doi.org/10.1016/j.bios.2017.02.054>.

[26] Shekari, Z. Zare, H. R., Falahati, A. 2021. Dual assaying of breast cancer biomarkers by using a sandwich-type electrochemical aptasensor based on a gold nanoparticles-3D graphene hydrogel nanocomposite and redox probes labeled aptamers, *Sensors & Actuators: B. Chemical* 332 (2021) 129515. <https://doi.org/10.1016/j.snb.2021.129515>.

[27] Samira Yazdanparast, Ali Benvidi, Mostafa Azimzadeh, Marzieh Dehghan Tezerjani & Mohammad Reza Ghaani. Experimental and theoretical study for miR-155 detection through resveratrol interaction with nucleic acids using magnetic core-shell nanoparticles. *Microchim Acta* 187, 479 (2020). <https://doi.org/10.1007/s00604-020-04447-9>

[28] Miller, J.N., Miller, J.C. *Statistics and Chemometrics for Analytical Chemistry*, 6th ed., Pearson Education, UK, 2018.

[29] Haghparas, Z., Kordrostami, Z., Sorouri, M. et al. Highly sensitive non-enzymatic electrochemical glucose sensor based on dumbbell-shaped double-shelled hollow nanoporous CuO/ZnO microstructures. *Sci Rep* 11, 344 (2021). <https://doi.org/10.1038/s41598-020-79460-2>

[30] Arif Dooa, Hussain Zakir, Sohail Manzar, Liaqat Muhammad Arman, Khan Muzamil Ahmad, Noor Tayyaba, A Non-enzymatic Electrochemical Sensor for Glucose Detection Based on Ag@TiO₂@ Metal-Organic Framework (ZIF-67) Nanocomposite, *Frontiers in Chemistry*, 8 (2020) 845. DOI=10.3389/fchem.2020.573510

[31] Palsaniya, S.; Nemade, H.B.; Dasmahapatra, A.K. Mixed Surfactant-Mediated Synthesis of Hierarchical PANI Nanorods for an Enzymatic Glucose Biosensor. *ACS Appl. Polym. Mater.* 2019, 1, 647–656.

[32] Comba, F.N.; Romero, M.R.; Garay, F.S.; Baruzzi, A.M. Mucin and carbon nanotube-based biosensor for detection of glucose in human plasma. *Anal. Biochem.* 2018, 550, 34–40.

[33] Esmaeeli, A.; Gha_arinejad, A.; Zahedi, A.; Vahidi, O. Copper oxide-polyaniline nanofiber modified fluorine doped tin oxide (FTO) electrode as non-enzymatic glucose sensor. *Sens. Actuators B Chem.* 2018, 266, 294–301.

[34] Ghanbari, K.; Babaei, Z. Fabrication and characterization of non-enzymatic glucose sensor based on ternary NiO/CuO/polyaniline nanocomposite. *Anal. Biochem.* 2016, 498, 37–46.

[35] Liu, X.; Long, L.; Yang, W.; Chen, L.; Jia, J. Facilely electrodeposited coral-like copper micro-/nano-structure arrays with excellent performance in glucose sensing. *Sens. Actuators B Chem.* 2018, 266, 853–860.

[36] Dai Z, Yang A, Bao X, Yang R. Facile Non-Enzymatic Electrochemical Sensing for Glucose Based on Cu₂O-BSA Nanoparticles Modified GCE. *Sensors (Basel)*. 2019;19(12):2824. Published 2019 Jun 24. doi:10.3390/s19122824.

[37] A. Mohamed Azharudeen, R. Karthiga, M. Rajarajan, A. Suganthi, Fabrication, characterization of polyaniline intercalated NiO nanocomposites and application in the development of non-enzymatic glucose biosensor, *Arabian Journal of Chemistry*, 13, Issue 2, 2020, 4053-4064. <https://doi.org/10.1016/j.arabjc.2019.06.005>.

[38] El-Ebidi AM, Saleem TH, Saadi MGE, Mahmoud HA, Mohamed Z, Sherkawy HS. Cyclophilin A (CyPA) as a Novel Biomarker for Early Detection of Diabetic Nephropathy in an Animal Model. *Diabetes Metab Syndr Obes.* 13 (2020) 3807-3819. <https://doi.org/10.2147/DMSO.S260293>

Figure Caption

Scheme 1. Schematic diagram for fabrication of proposed nanobiosensor for detection of miR-375 in detection of diabetes.

Figure. 1. TEM images of the A) GO and B) GNU, FESEM images of the SPCE modified with C) GO, E) GNU/GO hybrid, D) EDX Analysis of the proposed electrochemical sensor.

Fig. 2. Cyclic voltammograms of the modified SPCE in 0.1 mM $[\text{Fe}(\text{CN})_6]^{3-/4-}$ in 0.1M KCl for bare SPCE (a), GO/SPCE (b), GNU/GO/SPCE (c), MCH/ssDNA/GNU/GO/SPCE (d) and dsDNA/GNU/GO/SPCE (e).

Figure 3. Changes of Analytical signal of Probe versus concentration fixed GO on SPCE.

Figure 4. Changes of Analytical signal of Probe versus concentration fixed GNU on SPCE.

Figure 5. DPVs of Hem accumulated on the SPCE surface (as probe) before hybridization: a) immobilization of the probe by self-assembly in solution. b) immobilization of the probe by small droplet self-assembly method. c) Hybridization after immobilization of the probe by self-assembly in solution. d) Hybridization after probe immobilization by small droplet self-assembly method.

Figure 6 - Changes in current response of hematoxylin versus probe concentration.

Figure 7 - Changes in current response of accumulated Hem versus immobilization time of probe.

Figure 8 - Changes in current response versus Hem concentration.

Figure 9- Current changes versus time used to accumulate Hem at dsDNA/GNU/GO/SPCE.

Figure 10. DPVs of accumulated Hem on SPCE modified with ds- probe using Hybridization method, a) small droplet method, b) preheated solution and c) in solution.

Figure. 11. Assessment of the nanobiosensor selectivity by comparing DPVs of the Hem accumulating for 60 min on the (a) nanobiosensor incubated in complementary target miR-200b without applying the OB, (b) only MCH treated on the GNR/GO modified GCE, (c) non-hybridized nanobiosensor (SS-Probe/MCH/GNR/GO/GCE), (d) nanobiosensor incubated in non-complementary target, (e) nanobiosensor incubated in three-base mis match target, (f) nanobiosensor incubated in one-base mismatch target, and (g) nanobiosensor incubated in complementary target miR- 200b with applying Hem

Figure. 12. (A) DPVs of Hem accumulated on the hybridized ssDNA/GNU/GO/SPCE with different concentrations of the complementary (target) DNA in a 0.1 M phosphate buffer solution (pH 7.0) for 2 h. The numbers of 1–10 correspond to 0.2–800 pM target DNA. Inset (B) shows the plot of difference in the accumulated Hem current response on ssDNA/GNU/GO/SPCE versus the target DNA concentration in the hybridization process.

Scheme 1.

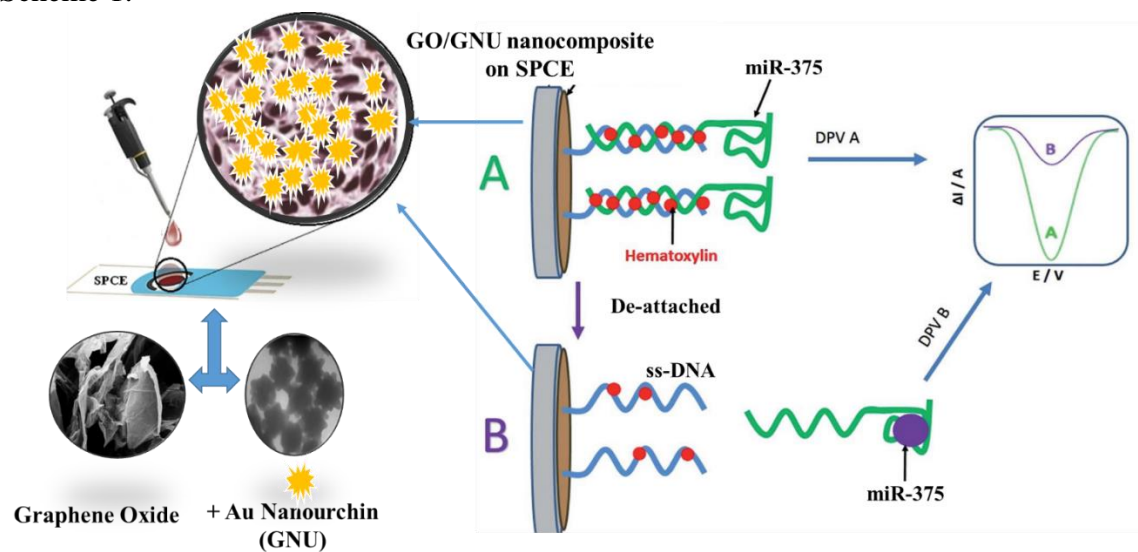


Figure. 1.

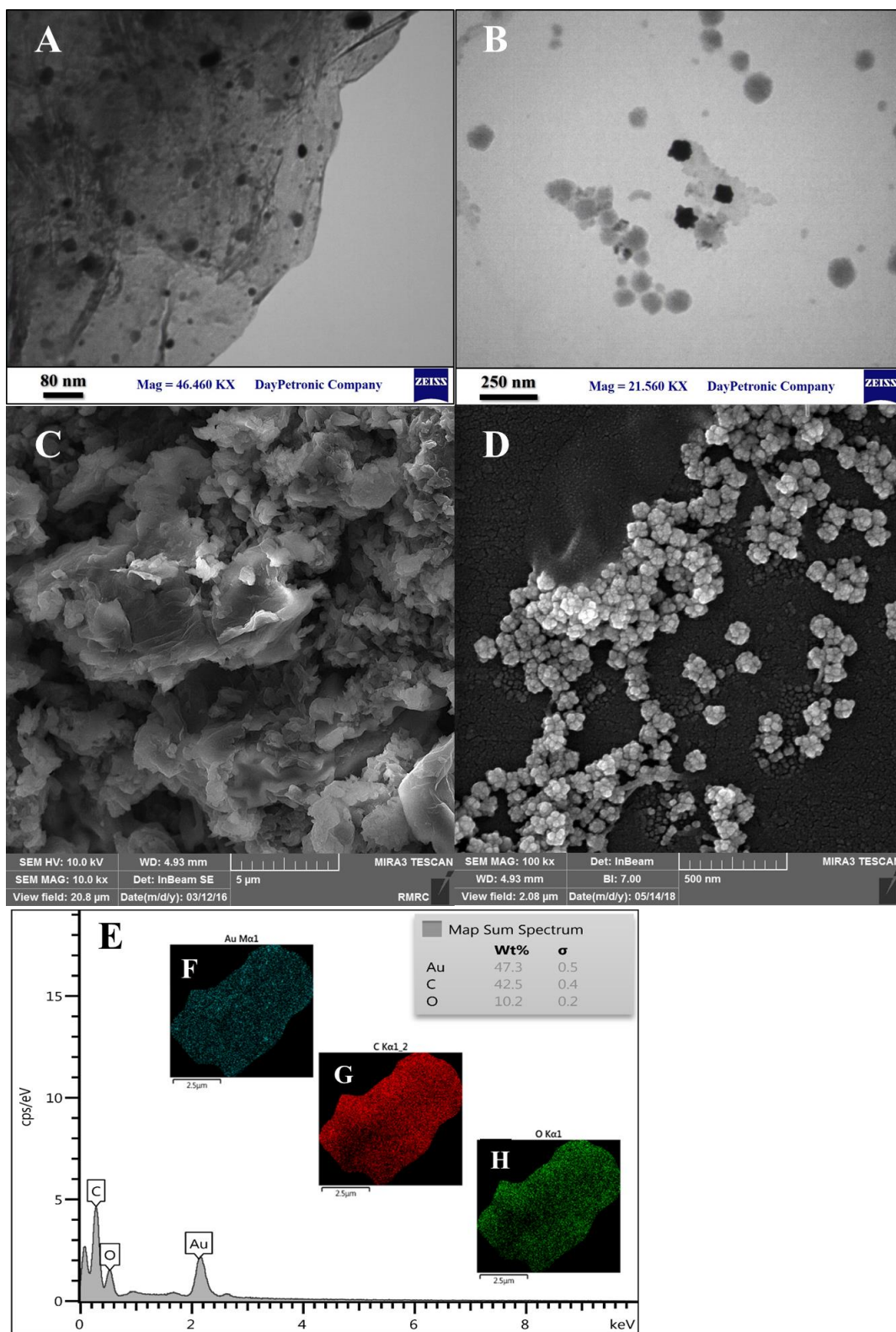


Figure 2.

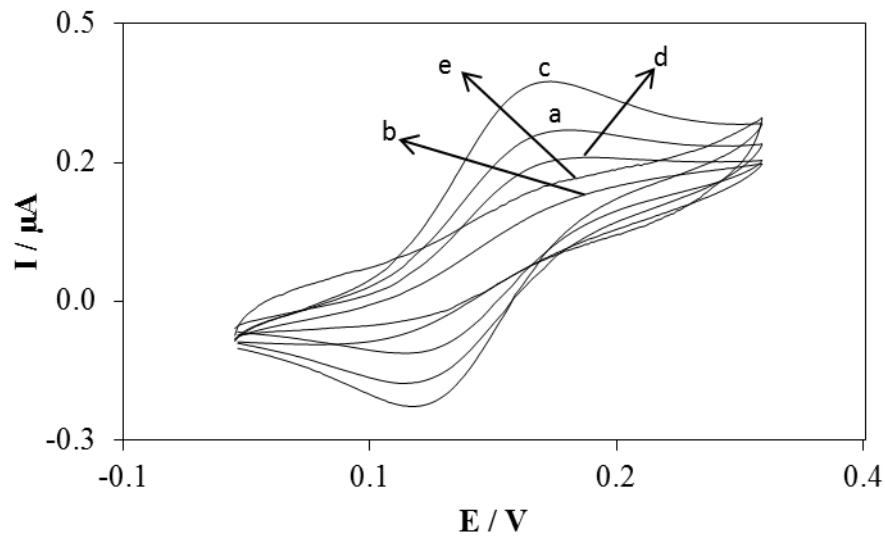


Figure 3.

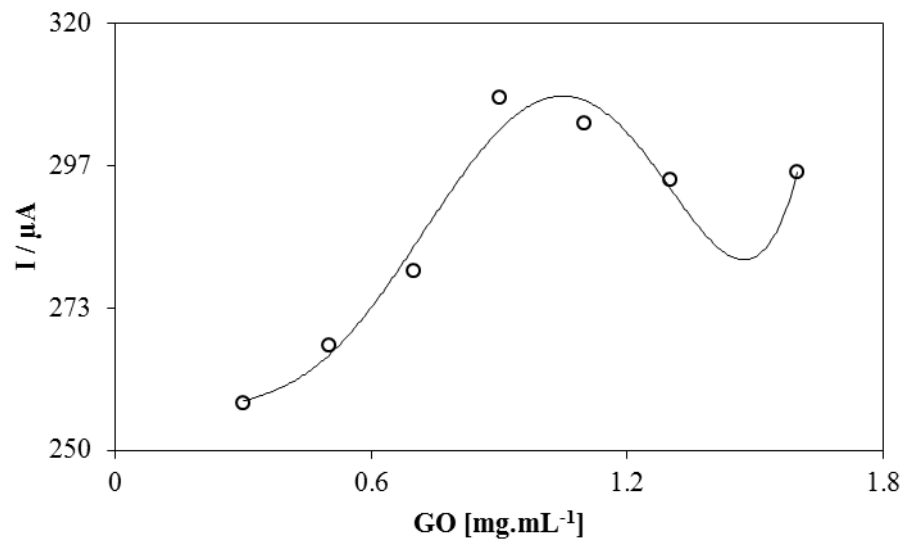


Figure 4.

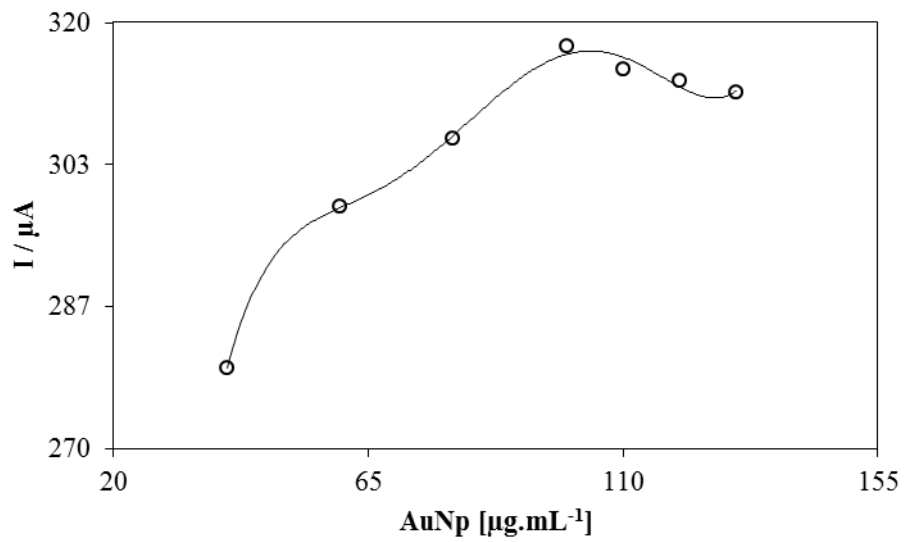


Figure 5.

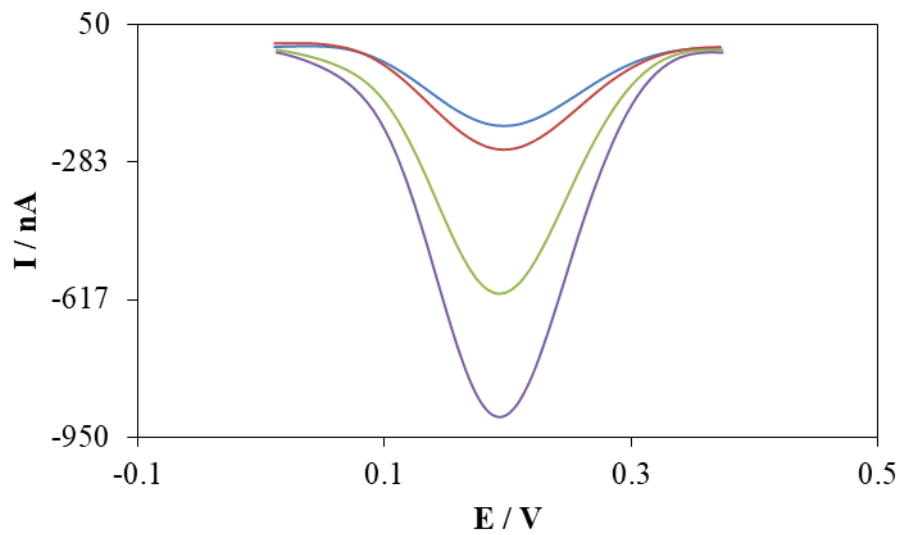


Figure 6.

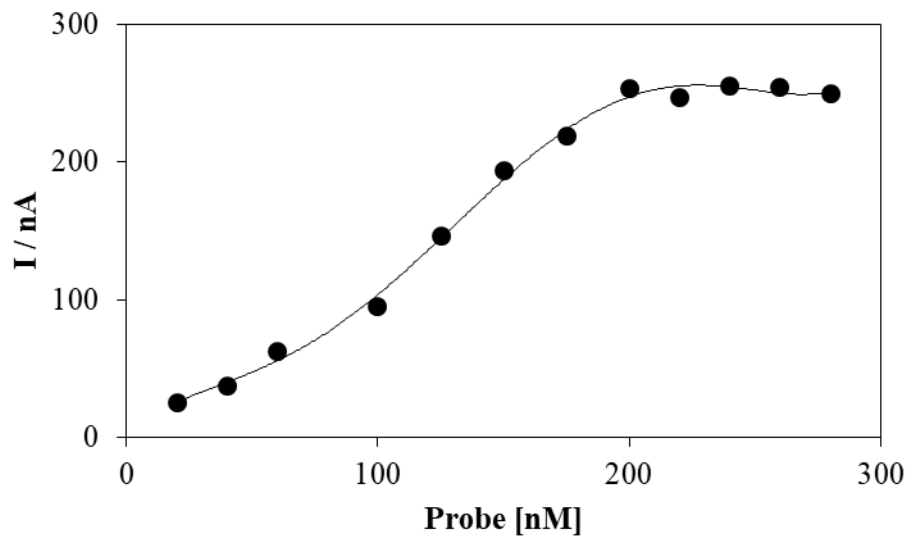


Figure 7

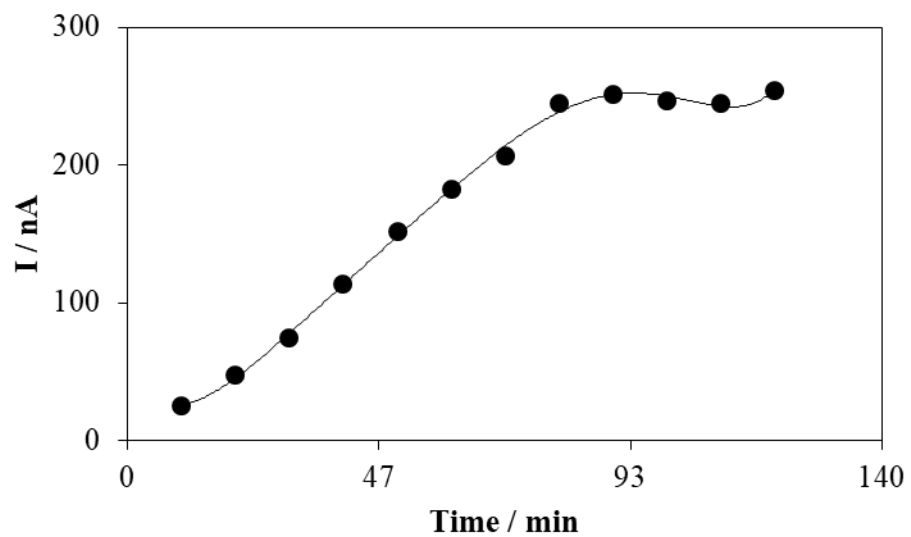


Figure 8

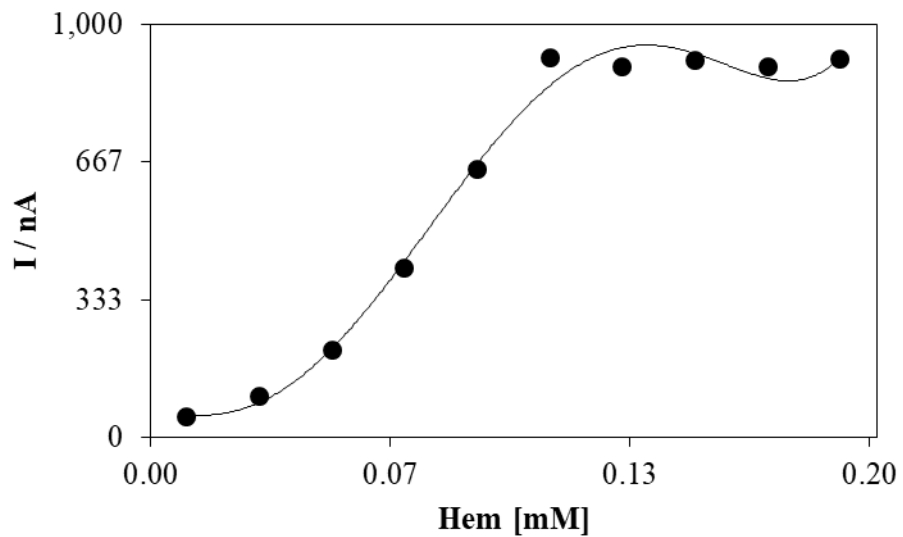


Figure 9 .

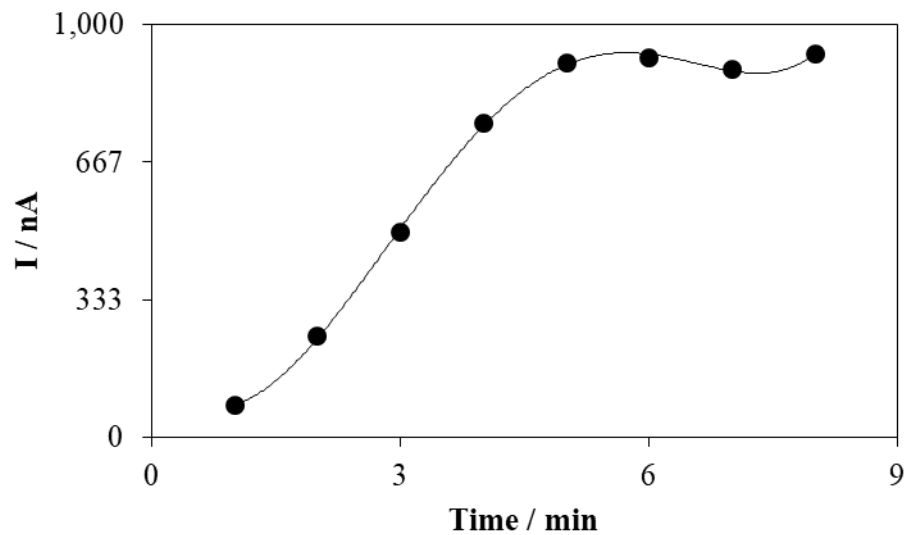


Figure 10.

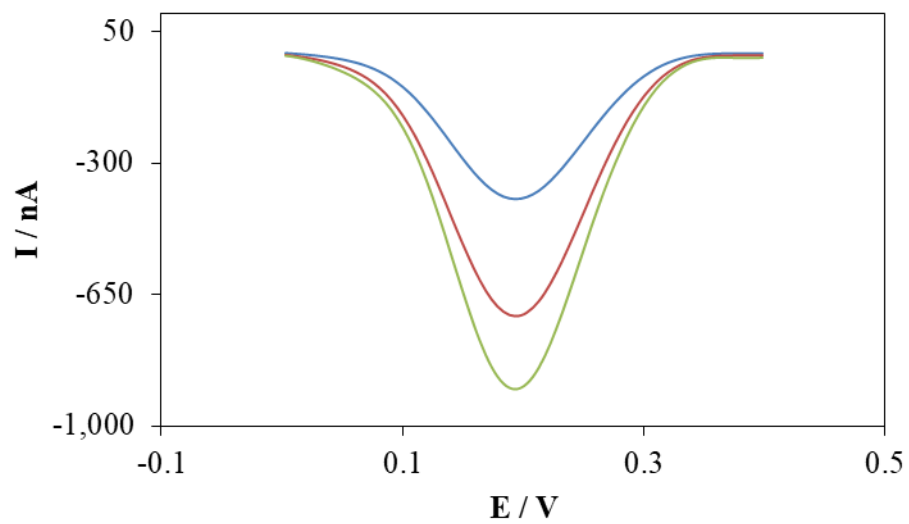


Figure 11.

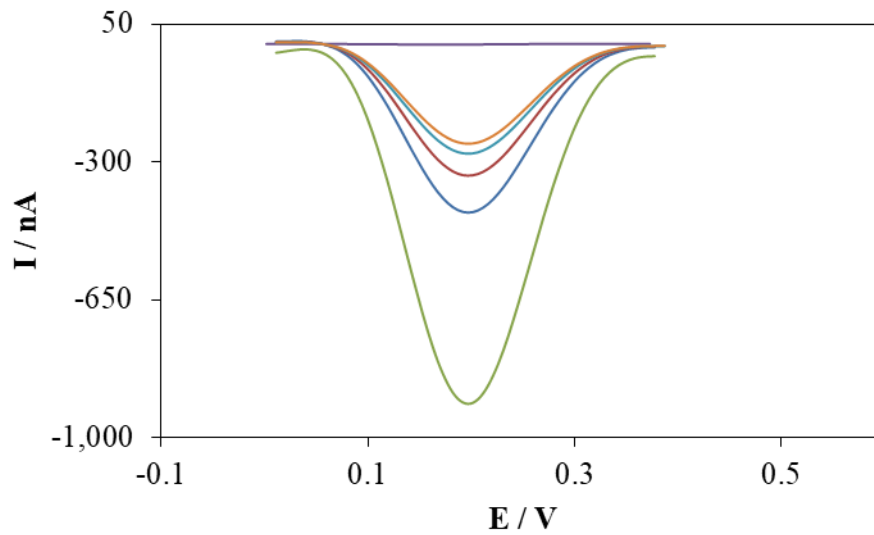


Figure. 12.

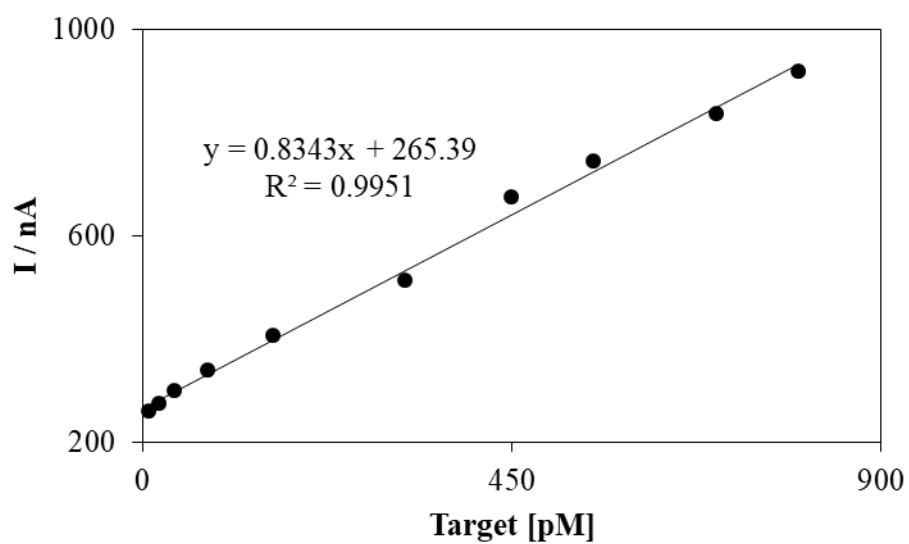
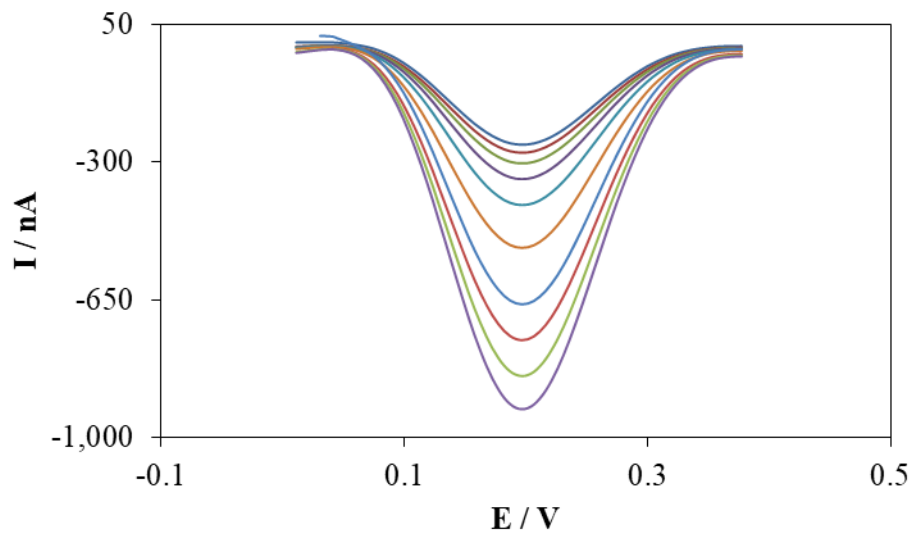


Table 1- List of the used chemicals

No.	Chemicals	Abbr.	Manufacture	Purity (%)
1	Graphene Oxide	GO	Sigma Aldrich	99
2	6-Mercapto-1-hexanol	MCH	Sigma Aldrich	97
3	Hematoxylin	Hem	Merck, Germany	98
4	Gold nanourchin	GNP	Sigma Aldrich	99.99
5	Ortho phosphoric acid	PA	Merck, Germany	98
6	Sodium Hydroxide	SH	Merck, Germany	97.5
7	Sodium Chloride	SC	Sigma Aldrich	98
8	K ₃ [Fe(CN) ₆]	-	Sigma Aldrich	99
9	Tris hydrochloride	Tris-Hcl	Sigma Aldrich	99
10	Ethylene diamine tetra acetic acid	EDTA	Sigma Aldrich	98.5
11	Sulfuric acid	SA	Sigma Aldrich	99.99

Table 2 - Comparison of the analytical parameters of different biosensors for diabetes determination.

Indicator	Modifier	Electrode	Analyte	L. R.	D. L.	Ref
Hem	GNU/GO	SPCE	miR-375	0.2 – 800 pM	0.05 pM	This Work
Nafion	CuO/ZnO-DSDSHNM	GCE	Glucose	0.5 – 100 mM	375 nM	[29]
-	Ag@TiO ₂ @ZIF-67	GCE	Glucose	0.048 – 1.0 mM	0.98 μM	[30]
-	PANI-SDS-F127(1:1)/GOx	GCE	Glucose	5.0 -50.0 mM	3.2 μM	[31]
-	Pt-CNT-muc 50%	GCE	Glucose	0.002 – 3.2 mM	3.0 μM	[32]
-	CuO/PANI-NF/FTO	GCE	Glucose	0.00025 - 0.28 & 0.28-4.8 mM	0.24 μM	[33]
-	CuO/NiO/PANI	GCE	Glucose	20.0- 2500 μM	2.0 μM	[34]
-	coral-like Cu micro-/nano-structure arrays	GCE	Glucose	0.2 μM - 1.90 mM	0.04 μM	[35]
Nafion	Cu ₂ O-BSA	GCE	Glucose	up to 10 mM	0.4 μM	[36]
	NiO/PANI	GCE	Glucose	Up to 100 μM	0.19 μM	[37]

Table 3. Results of the real sample study for designed sensor and comparing with the PCR method

Sample	Detected in [fM]	Spiked [fM]	Detected by QRT-PCR	Measured [fM]	Recovery %
Blank	<DL	40	40.2	40.5	101.25
		80	80.3	79.7	99.62
		120	120.7	122	101.66
Healthy person	<DL	40	40.3	39	97.5
		80	80.2	81.7	102.12
		120	120.5	118.54	98.78
A person with diabetes	50	40	90.4	90.7	101.77
		80	130.5	128.6	98.92
		120	170.7	172.6	101.52